

LA--11918-MS

DE91 001048

*New Multiphase  
Equation of State  
for Polycrystalline Quartz*

*J. C. Boettger  
S. P. Lyon*

**MASTER**

**LOS ALAMOS** Los Alamos National Laboratory  
Los Alamos, New Mexico 87545

# NEW MULTIPHASE EQUATION OF STATE FOR POLYCRYSTALLINE QUARTZ

by

J. C. Boettger and S. P. Lyon

## ABSTRACT

We have generated separate equations of state (EOS's) for the alpha quartz, coesite, and stishovite phases of polycrystalline quartz ( $SiO_2$ ), using the computer program GRIZZLY. We also have modified the program GRIZZLY to combine two single-phase EOS's for a given material into a single two-phase EOS via minimization of the Gibbs free energy. This new version of GRIZZLY has been used to generate a three-phase SESAME type EOS for polycrystalline quartz using the three EOS's mentioned above. All four of the EOS's produced for  $SiO_2$  are now available on request.

---

## I. INTRODUCTION

Polycrystalline quartz ( $SiO_2$ ) is a material which has been of recurring interest to many users of the SESAME equation of state (EOS) library. This interest is mostly due to the large abundance of naturally occurring quartz in rocks. Unfortunately, the usefulness of any SESAME type EOS for quartz in hydrodynamic calculations is limited by the implicit assumption that any process considered will be reversible. In fact, it is well known that the alpha  $\rightarrow$  stishovite phase transition in quartz exhibits considerable hysteresis due to metastability of the alpha phase well above the equilibrium phase boundary.<sup>1</sup> This effect may be of crucial importance in hydrodynamic calculations involving shock loading through the metastable region followed by adiabatic release. The only way such an irreversible phase transition could be described realistically is by constructing separate EOS's for each phase of a given material and then switching between the single-

phase EOS's in some thermodynamically self-consistent fashion.

The task of describing irreversible phase transitions thus may be divided into two parts: (1) generating high quality global EOS's for all phases involved which are compatible in form and share a common zero of energy, and (2) developing a simple means of determining when and how to switch between the various phases. In general, the latter part remains an unsolved problem. (Swegle<sup>1</sup> has recently looked at this problem in great detail for several materials of geological importance including quartz.) There is however one special case in which the solution to this problem is known, i.e. the equilibrium case. Under the constraint of thermodynamic equilibrium, all of the phase transitions will be reversible and can be described by a multiphase EOS formed by combining the single-phase EOS's in such a way as to minimize the Gibbs free energy as a function of pressure.

In this investigation, we have used the program GRIZZLY<sup>2</sup> to generate global EOS's for the alpha quartz, coesite, and stishovite phases of  $SiO_2$ . These individual EOS's were then used to form an equilibrium multiphase EOS for  $SiO_2$ . The parameters used to generate the single-phase EOS's were adjusted to ensure that the final EOS reproduces the experimentally determined equilibrium phase boundaries. Thus, the single-phase EOS's should provide reliable input to more general multiphase calculations. In addition, the equilibrium EOS for quartz should provide a good reference for studying the nonequilibrium effects in dynamic processes via calculations similar to those done by Swegle.<sup>1</sup> Hopefully, such calculations will allow us to develop systematic techniques for using the single-phase EOS's to describe general nonequilibrium processes.

In the next section, we will describe the methods used to generate single- and multiphase EOS's in this investigation. In Section III, the single-phase EOS calculations are discussed in detail. The equilibrium multiphase EOS for quartz is described in Section IV.

## II. METHODOLOGY

Most of the EOS's in the SESAME library are partitioned into three terms for the pressure  $P$ , the internal energy  $E$ , and the Helmholtz free energy  $A$ :

$$P(\rho, T) = P_s(\rho) + P_n(\rho, T) + P_e(\rho, T) \quad (1)$$

$$E(\rho, T) = E_s(\rho) + E_n(\rho, T) + E_e(\rho, T) \quad (2)$$

$$A(\rho, T) = A_s(\rho) + A_n(\rho, T) + A_e(\rho, T) \quad (3)$$

where  $\rho$  is the density and  $T$  is the temperature. (In the SESAME library, discrete values of  $\rho$  and  $T$  are chosen to form a mesh on which  $P$ ,  $E$ , and  $A$  are stored.) The subscripts  $s$ ,  $n$ , and  $e$  denote the contributions due to the static lattice (i.e. frozen nuclei) cold curve (zero temperature isotherm), the nuclear motion, and the thermal electronic excitations. It is thus possible to treat each contribution independently using any desired model. The free energy  $A$  can be related to the energy as:

$$A(\rho, T) = E(\rho, T) - T S(\rho, T) \quad (4)$$

where  $S$  is the entropy.

In the computer program GRIZZLY,<sup>2</sup> the only model available for calculating the electronic contributions is the Thomas-Fermi-Dirac (TFD) model.<sup>3</sup> In our calculations, we first generated electronic EOS's for each constituent atom. These monatomic electronic EOS's were then combined via additive volume mixing<sup>2</sup> to form the electronic EOS of  $SiO_2$ . This part of the calculation requires the atomic numbers (Si - 14, O - 8) and the atomic masses (Si - 28.086, O - 15.999) for the constituent atoms.<sup>4</sup>

The nuclear contributions were obtained using the CHARTJD nuclear model<sup>5</sup> (a modified version of the CHARTD model)<sup>6</sup> with a Gruneisen function of the CHARTD form.<sup>6</sup> In this model, the material is treated as a Debye solid at low temperatures and as an ideal gas at high

temperatures. The nuclear contribution switches smoothly between these two limits for temperatures near the melt. In addition to the data already specified, the nuclear calculation requires the reference density ( $\rho_0$ ), the Debye temperature ( $\Theta_D$ ), the reference Gruneisen constant ( $\gamma_0$ ), and the melt temperature ( $T_m$ ).

The cold curves used here were obtained in the compressed region by removing thermal contributions from an input Hugoniot at modest compressions ( $< 1.5$ ) and then extrapolating to a mixed TFD cold curve at large compressions. This procedure ensures that the total EOS will reproduce the input Hugoniot and will have the correct large  $\rho$  behavior. In the expanded region ( $\rho < \rho_0$ ), the cold curves were forced to have a generalized Lennard-Jones form<sup>2</sup> constrained to smoothly connect with the compressed cold curve and to have the correct cohesive energy ( $E_c$ ). Besides the data already mentioned, this part of the calculation requires an input Hugoniot in the form of shock velocity ( $u_s$ ) vs particle velocity ( $u_p$ ) (here in the form  $u_s = c + s u_p$ ) and a parameter FACLJ (here 1.0) which determines the shape of the cold curve in the expanded region.

For this investigation, we have modified GRIZZLY to allow two EOS's to be combined in such a way as to minimize the Gibbs free energy as a function of pressure. The Gibbs free energy may be expressed as

$$G(P, T) = A(\rho, T) + P/\rho. \quad (5)$$

Given two EOS tables for a low pressure phase (table 1) and a high pressure phase (table 2), the new command (PHASE 1 2 3 pcut /) directs GRIZZLY to search each isotherm (using the temperature grid of table 1) for the pressure  $P_t(T)$  at which the Gibbs free energies of the two EOS's are identical. The densities  $\rho_1$  and  $\rho_2$  at which the pressures for the two EOS's equal  $P_t$  form the boundaries of the mixed phase region in  $(\rho, T)$  space. The combined EOS is then formed and stored in table 3 using the  $T$  and  $\rho$  grids from table 1. Table 3 is identical to table 1 for  $\rho < \rho_1$  and is obtained directly from table 2 for  $\rho > \rho_2$ . In the mixed phase region, table 3 is obtained by setting  $P = P_t$  and assuming that for a given density the fractional amounts of the two phases ( $w_1$

and  $w_2$ ) are given by

$$w_1 = [(\rho_2 - \rho) / (\rho_2 - \rho_1)] (\rho_1 / \rho) \quad (6)$$

and

$$w_2 = [(\rho_1 - \rho) / (\rho_1 - \rho_2)] (\rho_2 / \rho). \quad (7)$$

To ensure that the phase boundary is described correctly, we used an enriched density grid in the mixed phase region. For high densities, it is possible to obtain spurious transitions due to the relatively sparse grid used in that region. To avoid that difficulty, we restricted the search on the zero temperature isotherm to pressures less than PCUT (a new input variable with a default value of 10 Mbar). For each higher temperature isotherm, the upper density for the search on table 1 is set at 5 grid points above the  $\rho_1$  obtained for the previous isotherm. For each isotherm, GRIZZLY begins its search at the high density limit and searches down for the first transition. This procedure ensures that GRIZZLY will not find spurious transitions or switch from one phase boundary to another.

### III. SINGLE-PHASE EOS

The various parameters used as input to GRIZZLY for the alpha, coesite, and stishovite phases of quartz are given in Table 1. The input data for the alpha phase was chosen to be consistent with that used in generating SESAME EOS 7383 (polycrystalline quartz),<sup>7</sup> except for  $T_m$  which is taken from a standard reference source.<sup>8</sup> The values of  $\rho_0$ ,  $\gamma_0$ , and  $c_0$  (as deduced from the bulk modulus) for the coesite and stishovite phases are taken from Davies.<sup>9</sup> The slope of the Hugoniot for the stishovite phase is that derived by McQueen, et al.<sup>10</sup> from Hugoniot data for polycrystalline quartz and fused quartz. That value was also used for coesite in the absence of any empirical data. The values of  $T_m$  for the high pressure phases were constrained to be twice the value of  $\Theta_D$ .

(Our results are relatively insensitive to the choice of  $s$  for coesite and  $T_m$  for both coesite and stishovite.)

Table 1: Single Phase EOS Parameters

	alpha	coesite	stishovite
$\rho_0$ (gm/cc)	2.65	2.91	4.29
$\gamma_0$	0.65	0.40	1.22
$\theta_D$ (K)	950	986	1210
$E_c$ (kcal/mole)	146.000	145.338	141.960
$C_0$ (km/s)	3.77	5.77	9.03
$S$	1.93	1.00	1.00
$T_m$ (K)	1900	1972	2420

The remaining parameters for the coesite and stishovite phases ( $\theta_D$  and  $E_c$ ) were used as adjustable parameters to match the experimental  $\alpha \rightarrow$  coesite<sup>11</sup> and coesite  $\rightarrow$  stishovite<sup>12</sup> phase boundaries (see Fig. 1). We began by generating the EOS for the alpha phase using the data given in Table 1. The EOS for the coesite phase was then generated for various values of  $\theta_D$  and  $E_c$ . For each set of values used, the EOS of coesite was combined with that of the alpha phase to obtain the phase boundary. We were quickly able to match the experimental boundary in  $P$  vs  $T$  space. We then repeated that procedure with the stishovite phase.

While the final value of  $\theta_D$  used for the stishovite phase (1210 K) is in reasonable agreement with the value quoted by Davies (1120 K),<sup>9</sup> the value found here for coesite (986 K) differs significantly (16%) from the experimental value (1170 K).<sup>9</sup> The poorer agreement found for the coesite phase may be due in part to the relative imprecision of the experimental determination of the  $\alpha \rightarrow$  coesite phase boundary.<sup>13</sup> However, this disagreement may also simply reflect the difficulties in rigorously defining a single temperature-independent  $\theta_D$  for any given material. (In general,  $\theta_D$  is merely a parameter used to fit data over some temperature range.) Assessing the

values of  $E_c$  used here for the high temperature phases is best done by comparison with the experimental ( $T=0, P=0$ ) energy differences between the various phases.<sup>13</sup> The alpha - stishovite energy difference obtained here is 12.120 kcal/mole (note that the values in Table 1 are for average atom moles and must be multiplied by 3) compared to an experimental value of 12.1 kcal/mole.<sup>13</sup> Again, the agreement with experiment is substantially poorer for the coesite phase. Here we obtain an alpha - coesite energy difference of 1.986 kcal/mole compared with the experimental value of 1.2 kcal/mole. This result suggests that there may in fact be some difficulty with the experimental alpha  $\rightarrow$  coesite phase boundary used to determine  $\theta_D$  and  $E_c$ .

To summarize, both the alpha and stishovite single-phase EOS's were generated using parameters which are either well determined experimentally or were selected to reproduce the experimental phase boundaries. Therefore, these two EOS's should be quite good. For the coesite phase, the parameters used are not as well determined experimentally as for the other phases. Hence, the quality of the coesite EOS is questionable. Fortunately, the coesite phase is believed to be of little importance for processes involving shock loading<sup>1</sup> and the questionable nature of the parameters used should not seriously effect our work.

#### IV. EQUILIBRIUM MULTIPHASE EOS FOR QUARTZ

The best means available for evaluating the quality of the three single-phase EOS's generated here is via the resulting equilibrium multiphase EOS for quartz. In Fig. 1, the equilibrium phase boundaries obtained here are compared with the experimental alpha  $\rightarrow$  coesite<sup>10</sup> and coesite  $\rightarrow$  stishovite<sup>11</sup> boundaries used in generating the single-phase EOS's. The high quality of the fit to the data is clearly evident. Figure 1 also includes the alpha  $\rightarrow$  stishovite phase boundary which would exist if the coesite phase were ignored. This hypothetical boundary is of great importance since it has been suggested that under shock conditions quartz transforms directly from a

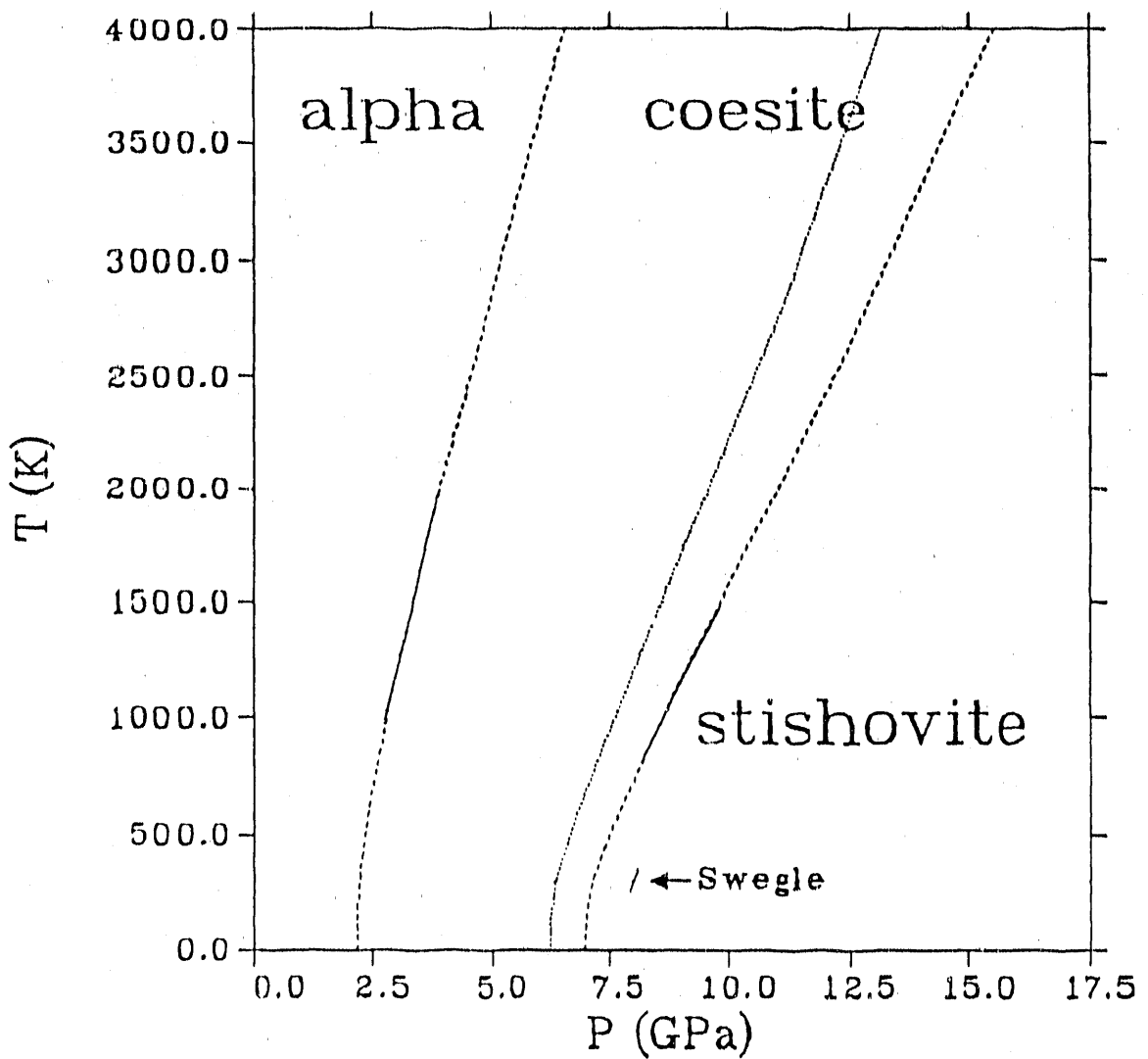


Fig. 1. The theoretical phase diagram for  $SiO_2$  (dashed lines) compared with the experimental  $\alpha \rightarrow$  coesite (Ref. 10) and coesite  $\rightarrow$  stishovite (Ref. 11) boundaries (solid lines). Also shown are the hypothetical  $\alpha \rightarrow$  stishovite boundary obtained here (dotted line) and that used by Swegle (Ref. 1).

metastable alpha phase to the stishovite phase.<sup>1</sup> In his investigation of the effects of metastability on dynamic processes in quartz, Swegle<sup>1</sup> assumed that the coesite phase is irrelevant. The alpha  $\rightarrow$  stishovite phase boundary used by Swegle<sup>1</sup> is included in Fig. 1. (He only reports the position and slope of the boundary at one point.) It is intriguing that the phase boundary used in that investigation differs from that obtained here by nearly 2 GPa (more than 20%) at room temperature. Whether or not that difference will substantially alter the estimated impact of metastability on dynamic processes in quartz remains to be seen.

Another important consideration for our purposes is the quality of the Hugoniot generated from the equilibrium multiphase EOS. In Figs. 2 and 3, the theoretical  $u_s$  vs  $u_p$  curve is compared with experimental data from a variety of sources.<sup>14-17</sup> Naturally, the portion of the curve prior to the first phase transition matches the input Hugoniot for the alpha phase and is guaranteed to be in good agreement with experiment. This is not true for the portions of the Hugoniot which involve the coesite or stishovite phases since the initial conditions differ from those of the input Hugoniots used to construct the EOS's for those phases. For  $u_p > 2.5$  km/s, the theoretical Hugoniot is in excellent agreement with the experimental data, demonstrating the high quality of the stishovite EOS used in generating the multiphase EOS. In fact, the large  $u_p$  portion of the curve is substantially better than that produced by SESAME EOS 7383,<sup>7</sup> since that EOS was generated by inputting a  $u_s$  vs  $u_p$  curve constructed out of straight-line segments and thus cannot reproduce the curvature of the experimental data.

In Fig. 4, we show part of the calculated vs experimental Hugoniot in  $P$  vs  $\rho$  space. This figure clearly reveals the large difference between real shock processes in quartz as opposed to a hypothetical equilibrium process. For the experimental Hugoniot, the transition from the alpha phase begins at a pressure of about 14 GPa and the quartz has completely transformed to the stishovite phase at about 45 GPa.<sup>14</sup> Throughout the experimental transition, the pressure rises monotonically as a function of density. In contrast, the theoretical transition is composed of two

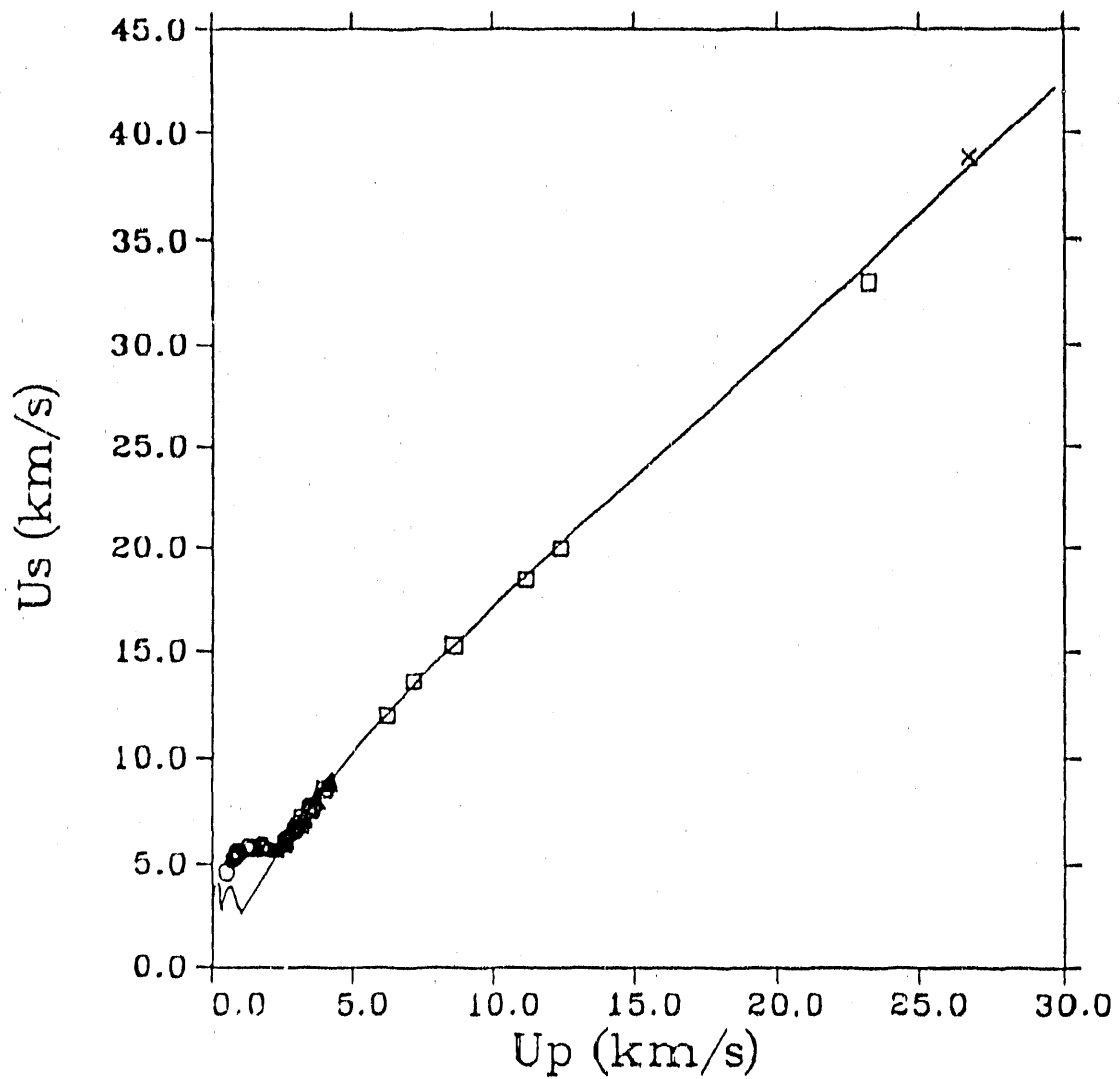


Fig. 2. Theoretical  $u_s$  vs  $u_p$  curve (line) compared with experiment (circles - Ref. 14, triangles - Ref. 15, squares - Ref. 16, crosses - Ref. 17). See Fig. 3 for a close up view of the small  $u_p$  region.

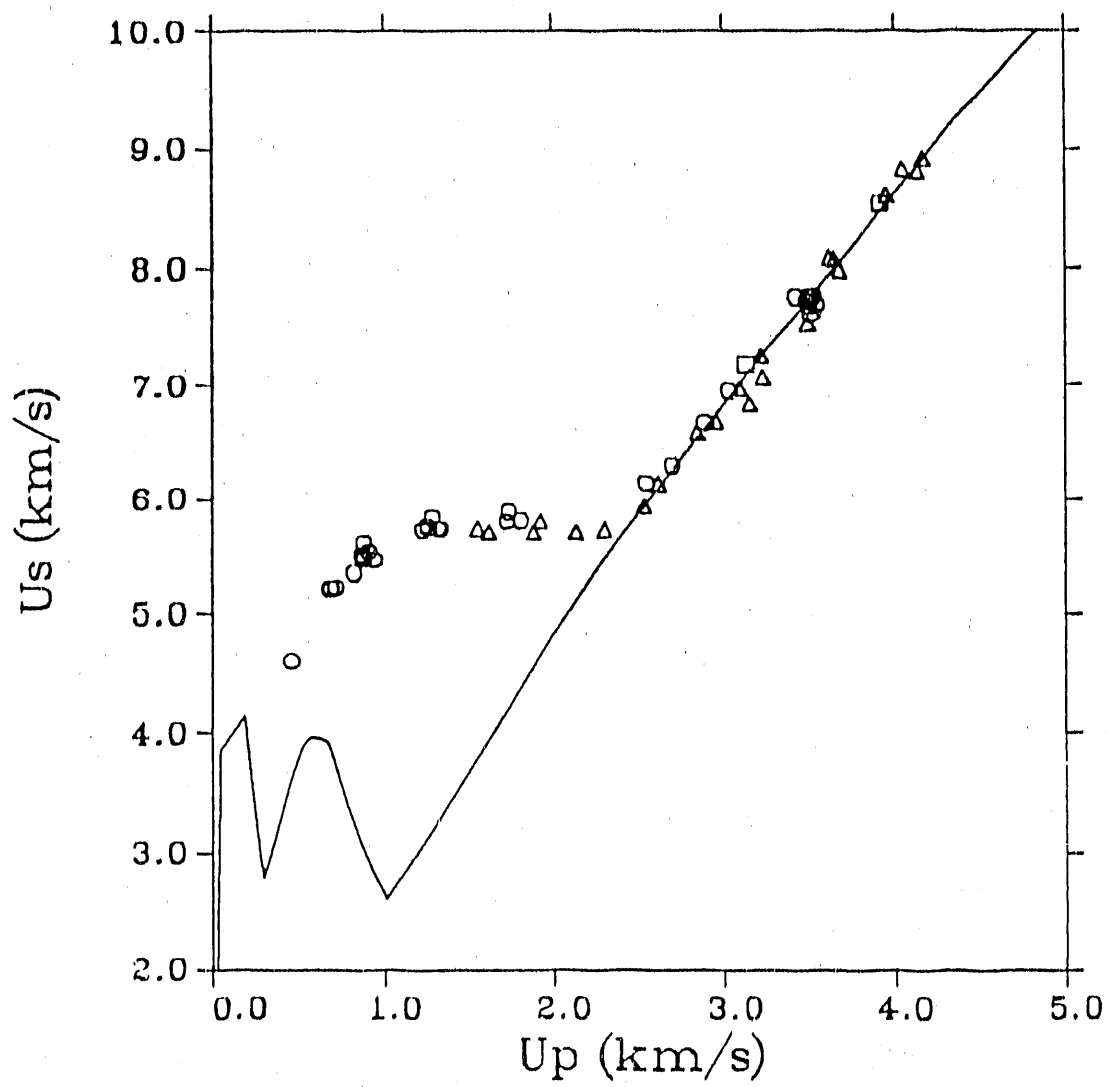


Fig. 3. Close up view of the small  $u_p$  region of Fig. 2.

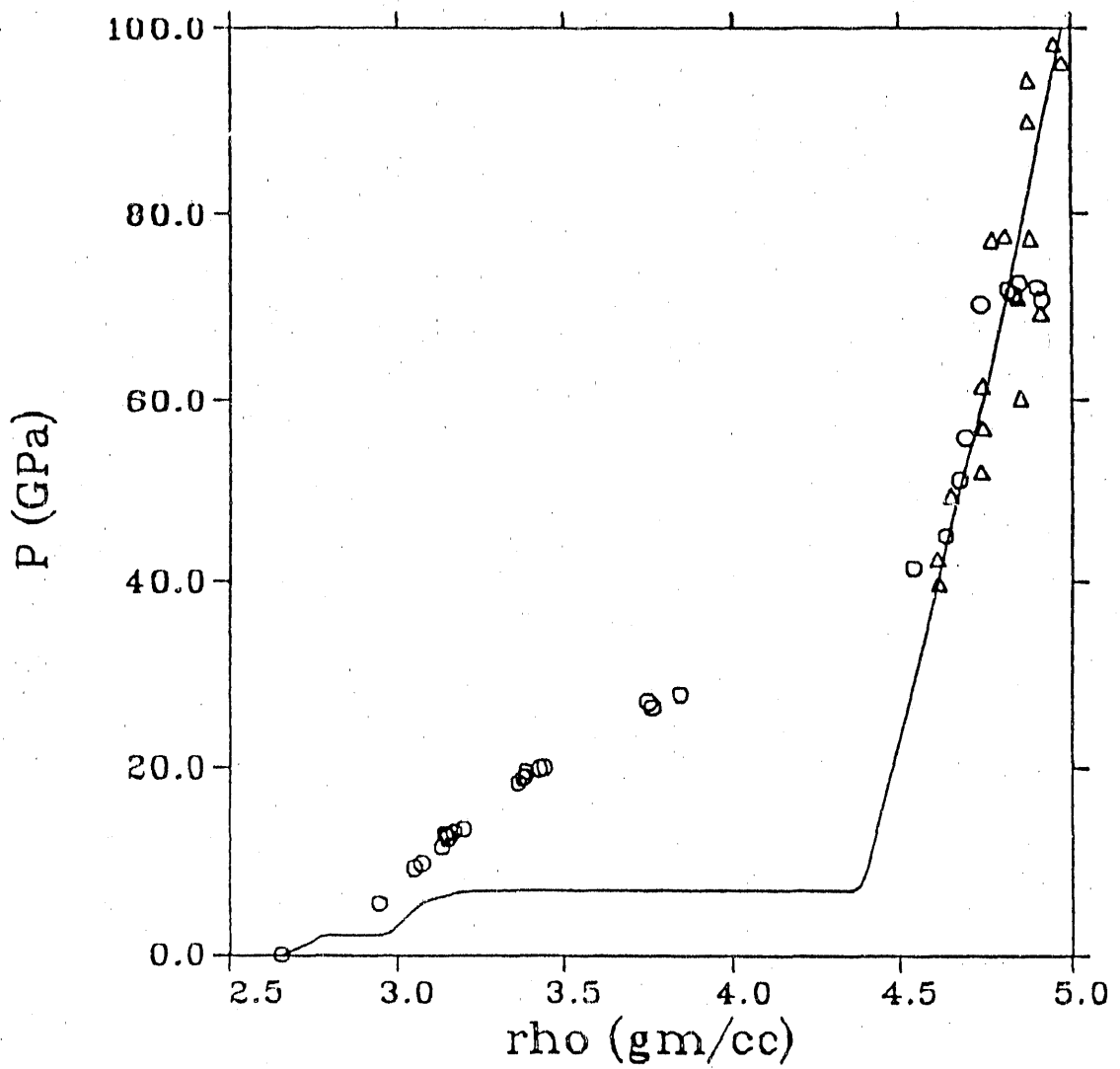


Fig. 4. Theoretical Hugoniot in  $P$  vs  $\rho$  space (line) compared with experiment (circles - Ref. 14, triangles - Ref. 15).

distinct transitions at constant pressure. The alpha  $\rightarrow$  coesite transition occurs at about 2.2 GPa and the coesite  $\rightarrow$  stishovite transition occurs at about 7.0 GPa.

Although the differences between the two curves in Fig. 4 are dramatic, no unambiguous interpretation of those differences can be given at this time, except that it is quite obvious that the alpha phase exhibits metastability for pressures between 2.2 GPa and 14 GPa. The problem in interpreting the remainder of the differences is that it is not clear that in the mixed phase region one can directly relate the measured values of  $u_s$  and  $u_p$  to  $P$  and  $\rho$  as is assumed in Fig. 4. Thus the experimental curve is questionable for pressures between 14 GPa and 45 GPa. A further difficulty in interpretation is the problem of determining what effects are due to metastability and which are due to strength. To resolve these questions, it will be necessary to complete the next phase of this investigation; performing calculations similar to those done by Swegle<sup>1</sup> using the single-phase EOS's produced here to match experimental data via nonequilibrium mixing.

## REFERENCES

1. J. W. Swegle, "Irreversible Phase Transitions and Wave Propagation in Silicate Geologic Materials," Sandia National Laboratories report SAND89-1443 (August 1989).
2. J. Abdallah, Jr., "User's Manual for GRIZZLY," Los Alamos National Laboratory report LA-10244-M (September 1984).
3. R. D. Cowan and J. Ashkin, "Extension of the Thomas-Fermi-Dirac Statistical Theory of the Atom to Finite Temperatures," *Phys. Rev.* **105**, 144 (1957).
4. N. W. Ashcroft and N. D. Mermin, *Solid State Physics* (Holt, Rinehart, and Winston, 1976).
5. J. D. Johnson, Los Alamos National Laboratory, unpublished notes, 1986-1987.
6. S. L. Thompson and H. S. Lauson, "Improvements in the Chart D Radiation-Hydrodynamic Code III: Revised Analytic Equations of State," Sandia National Laboratories report SC-RR-71 0714 (March

1972).

7. J. D. Johnson and S. P. Lyon, "EOS for Polycrystalline Quartz," Los Alamos National Laboratory report LA-10391 MS (May 1985).
8. *CRC Handbook of Chemistry and Physics*, 69th Ed., R. C. Weast, Ed. (CRC Press, Inc., Boca Raton, 1988).
9. G. F. Davies, "Equation of State and Phase Equilibria of Stishovite and a Coesitelike Phase from Shock-Wave and Other Data," *J. Geophys. Res.* **77**, 4920 (1972).
10. R. G. McQueen, J. N. Fritz, and S. P. Marsh, "On the Equation of State of Stishovite," *J. Geophys. Res.* **68**, 2319 (1963).
11. F. R. Boyd and J. L. England, "The Quartz-Coesite Transition," *J. Geophys. Res.* **65**, 749 (1960).
12. S. Akimoto and Y. Syono, "Coesite-Stishovite Transition," *J. Geophys. Res.* **74**, 1653 (1969).
13. J. L. Holm, O. J. Kleppa, and E. F. Westrum, "Thermodynamics of Polymorphic Transformations in Silica," *Geo. Cosmo. Acta* **31**, 2289 (1967).
14. J. Wackerle, "Shock-Wave Compression of Quartz," *J. Appl. Phys.* **33**, 922 (1962).
15. R. G. McQueen, J. N. Fritz, and J. W. Hopson, Los Alamos National Laboratory, unpublished work (1985).
16. L. V. Al'tshuler, N. N. Kalitkin, L. V. Kuz'mina, and B. S. Chekin, "Shock Adiabats for Ultrahigh Pressures," *Sov. Phys. JETP* **45**, 167 (1977) and L. V. Al'tshuler, R. F. Trunin, and G. V. Simakov, NASA translation TT F-10, 101.
17. C. E. Ragan, III, Los Alamos National Laboratory, unpublished work (1985).

**END**

**DATE FILMED**

11/08/90

